Int. J. Electrochem. Sci., 14 **(2019)** 3844 – 3855, doi: 10.20964/2019.04.06

International Journal of
ELECTROCHEMICAL
SCIENCE
www.electrochemsci.org

Facile Synthesis of Au Nanoparticles@Reduced Graphene Oxide Nanocomposition-Modified Electrode for Simultaneous Determination of Copper and Mercury Ions

Youzhi Yao

Wuhu Institute of Technology, Wuhu 241003, China.
E-mail: yaoyz@whit.edu.cn

Received: 28 October 2018 / *Accepted:* 26 January 2019 / *Published:* 10 March 2019

A highly efficient electrochemical sensor consisted by gold nanoparticles (Au NPs）loaded on reduced graphene oxide (RGO) nanosheets for Cu^{2+} and Hg^{2+} was developed. The electrochemical performances of as-prepared bare glassy carbon electrode (GCE), RGO/GCE, Au NPs@RGO/GCE were characterized by cyclic voltammetry (CV) and differential pulse voltammetry (DPV), respectively. The Au NPs@RGO/GCE exhibited an excellent sensitivity toward Cu^{2+} and Hg^{2+}. The results revealed that the detection limit of Cu^{2+} was 0.0015 μM and Hg^{2+} was 0.02 μM (S/N = 3). In addition, the Au NPs@RGO nanocomposite modified electrode was optimized and applied for practical water sample analysis with a satisfactory outcome. The electrochemical sensor based on Au NPs@RGO would be expected to expand the application field of heavy metal detection.

Keywords: Au nanoparticles, reduced graphene oxide, simultaneous determination, electrochemical sensor.

1. INTRODUCTION

In the past several decades, pollution caused by heavy metal ions has become a remarkable and serious problem. Excessive emission of heavy metal ions has a great impact on the sustainable development of human [1]. Among heavy metal ions, mercury pollution in the environment has been mainly caused by the emissions of human industrial production [2-4]. Hg^{2+} is considered as one of the most prevalent and important mercury pollutants. Even at low concentration, Hg^{2+} has a high affinity for thiol groups in proteins or enzymes, so it is extremely harmful to human health, which can cause many diseases such as tremor, headache, hearing and cognitive loss, hallucination and even death [5, 6]. Copper is one of the most widely used metal materials nowadays, and it is also one of the essential trace elements for human body. Cu^{2+} plays crucial roles in various biological processes besides Fe^{2+} and Zn^{2+}. However, if the amount of the copper ions exceeds the normal level for the cellular needs, it will lead to prion disease, amyloidal precipitation and neurodegenerative disorders [7]. Therefore, monitoring the levels of potentially toxic metal Cu^{2+} and Hg^{2+} is still desired. Building up tools of the convenient, flexible and highly sensitivity for detecting Cu^{2+} and Hg^{2+} in variety of cases has sparked interest in many researchers [8, 9].

Hence, various efficient and reproducible methods, including atomic absorption spectroscopy [10], surface-enhanced Raman spectroscopy [11], fluorescence sensors [12], and electrochemical sensors [13] were used to determinate Cu^{2+} and Hg^{2+}. Among these conventional methods, sophisticated apparatuses and tedious process were usually required, and time-consuming sample preparation steps were involved [14]. In contrast, electrochemical determination has glamorous advantages, for instance, unsophisticated equipment, short analysis time, less sample requirement and high sensitivity [15].

For an electrochemical sensor, its good catalytic ability depends on modified material. Reduced graphene has become one of the research focuses in electrochemistry material due to its abundant functional groups, larger surface area and capability to fast electron transfer. RGO is becoming a more interesting candidate compared to graphene oxide powder. In addition, attributed to the rich oxygen-containing functional groups on its surface, RGO can accelerate the electron transfer rate [16].

Gold nanoparticles possess many astonishing performances, such as good biocompatibility, unique optical, electrical and catalytic properties, which can be widely used in biomedicine, sensors, optoelectronic devices and catalysis [17],e.g.. Meanwhile, gold nanoparticles can improve the specific surface area and catalytic performance of nanocomposites, which can improve the sensitivity of electrochemical sensors [18]. In particular, the synergistic effect of good catalytic activity of Au NPs and fast charge transfer rate of RGO is more conducive to improving the sensitivity of electrochemical sensors. Previously, many reports revealed that Au/RGO nanocomposites had been fabricated, and electrochemical sensors based on the nanocomposites have high sensitivity [19-21]. However, most of Au/RGO nanocomposites has been synthesized by using complex process and additional surfactants [22].

Here, without binder and surfactants, we designed a simple method to synthesize nanocomposites by one-step reduction with N_2H_4 as reducing agent, and the preparing process is handy. The structure of the as-prepared Au/RGO was characterized by SEM and EDX in order to examine morphology and component in the nanocomposites. On that foundation, a new sensor based on Au NPs@RGO nanocomposite for the direct electrochemical determination of Cu^{2+} and Hg^{2+} was developed. The electrochemical behavior of two ions on the sensor of Au NPs@RGO/GCE was performed. The factors affecting the sensor were further optimized, such as pH, concentration of nanocomposite and scan rate. The electrochemical sensor has been applied to the determination of Cu^{2+} and Hg^{2+} metal ions in river and tap water samples. The results display that the sensor has good sensitivity.

2. EXPERIMENTAL SECTION

2.1 Materials and reagents

Sodium tetrachloroaurate (III) dihydrate ($NaAuCl_4 \cdot 2H_2O$, Au: 48-50%) was obtained from

Aladdin Biotechnology Co. Ltd. (Shanghai, China). Graphene oxide (GO) is synthesized by improved Hummer's method [23]. Various Acetate Buffer Solution (ABS) (0.1M NaAc, HAc) were prepared, and pH values were from 3 to 7. Other reagents were of analytical grade and deionized water was used throughout the experiment.

2.2 Instruments

The specimens of scanning electron microscope were conducted on S-4800 field emission scanning electron microanalyses, Hitachi, Japan. Measurements of Cyclic voltammetric (CV) and Differential pulse voltammetry (DPV) were performed by a CHI660D electrochemical workstation (Shanghai Chenhua Instrument Company, China) in a conventional three-electrode setup, which platinum wire (ϕ 1 mm) was used as a auxiliary electrode and Ag/AgCl was taken as a reference electrode. The pH values of ABS were measured by a CT-6023 pH meter.

2.3 Synthesis of Au NPs@RGO nanocomposite

Typically, 40 μL $NaAuCl_4$ solution (0.01 M) was injected into 20 mL GO solution (0.5 mg/mL) under vigorous stirring at room temperature for 30 min in order to have $NaAuCl_4$ thoroughly dispersed on the surface of GO, and the beaker containing the mixture was heated in water bath (50 ºC). During the process, excessive amounts of N_2H_4 (1 mL) were dropped into the mixture, and $AuCl_4^-$ and GO were reduced to form Au NPs@RGO nanocomposite. Stirring lasted 30 minutes, and finally the black mixture solution (12 mL) was obtained. The obtained Au NPs@RGO was sonicated, centrifuged and washed by doubly distilled water and absolute alcohol several times, and then dried precipitate was dispersed by ultrasound to form 10 ml solution for standby application. RGO without $NaAuCl_4$ was prepared simultaneously .

2.4 Fabrication of the modified electrode

Prior to fabrication of the sensor, GCE has undergone a series of treatments. First, GCE was polished with AL_2O_3 (0.05 μm), then cleaned by ultrasound in water and ethanol, and finally dried in oven for reserve. A certain amount of RGO was added into deionized water, and then dispersed thoroughly in 15 minutes by ultrasound to form a stable mixed solution. Au NPs@RGO/GCE modified electrodes were prepared by coating 8 μL of mixed droplets on the treated GCE surface with a microinjector and drying at room temperature. RGO/GCE modified electrodes were prepared under similar conditions.The whole assembly procedures were illustrated in Fig.1.

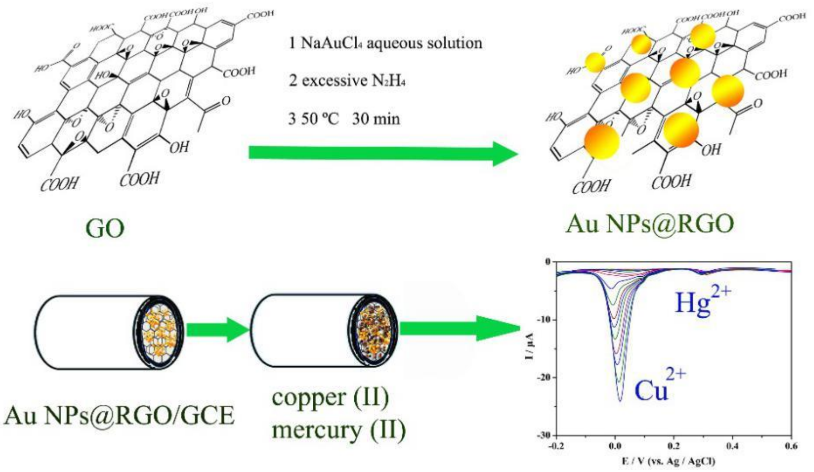

Figure 1. Schematic presentation for the synthesis by a one-step reduction approach, and the detection of Cu^{2+} and Hg^{2+} by DPV using an Au NPs@RGO modified GCE.

3. RESULTS AND DISCUSSION

3.1 Morphological and spectra characterization of Au NPs@RGO

The morphology of Au NPs@RGO was explored using SEM. The typical wrinkle morphology of RGO nanosheet is exhibited in Fig. 2a, and Au NPs with high density and well-dispersion(light spots) exhibited a regular spherical shape and uniformly loaded on the surface of RGO (Fig. 2b). It shows that GO and $NaAuCl_4$ were well reduced and stabilized the products successfully. Fig. 2c clearly indicated that the nanocomposites contained two main elements, Au and C, and peaks of other elements were due to the unwashed composite and substrate, and the amount of gold accounted for about 15% of the total mass of nanocomposites (showed in a table, Fig.1c, inset).

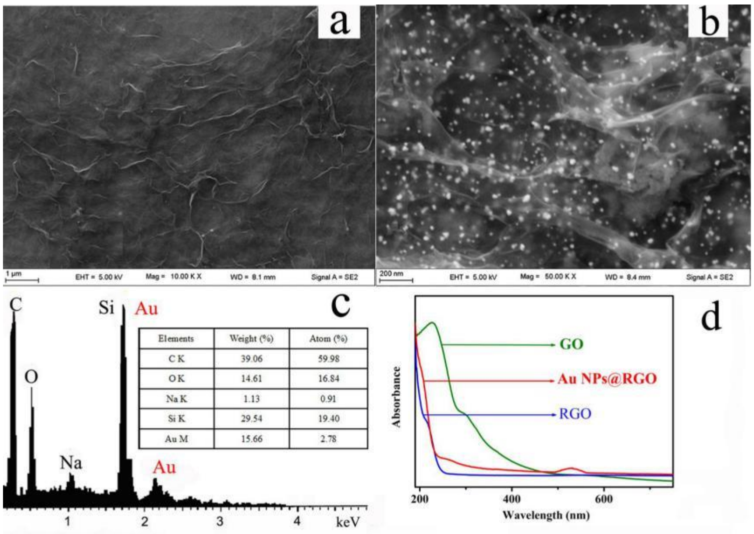

Elements	Weight (%)	Atom (%)
C K	39.06	59.98
O K	14.61	16.84
Na K	1.13	0.91
Si K	29.54	19.40
Au M	15.66	2.78

Figure 2. SEM images of RGO (a), Au NPs@RGO (b), EDX spectrum of Au NPs@RGO (c) and UV–vis spectroscopy of GO, RGO, and Au NPs@RGO (d). Inset, weight and atom percentages of elements found in spectrum.

GO, RGO and Au NPs@RGO were dispersed in aqueous solution and characterized by ultraviolet-visible spectroscopy, as shown in Fig.2 d. On the ultraviolet curve of GO, two characteristic peaks appeared, one was at 231 nm and the other was at 305 nm. The two characteristic peaks are caused by π–π* transitions of aromatic C-C bonds and n–π* transitions of C=O bonds, respectively [24]. The characteristic peak of RGO at 230 nm red-shifted to 265 nm, and the characteristic peak at 305 nm disappeared, which means that C=O was reduced. On the curve c of Au NPs@RGO, The characteristic peak at 230 nm further red-shifted to 270 nm, and another peak appeared at 530 nm, which is the characteristic absorption peak of gold [25]. All the results showed that RGO and Au NPs@RGO were successfully prepared.

3.2 Characterization of modified electrodes

Electron conductivity of modified electrode surface can be generally characterized by Electrochemical impedance spectroscopy (EIS), which is a simple and efficient method. The spectrum of EIS includes two parts, one is a linear portion at lower frequency range controlled by the diffusion-limited process, the other is a semicircle at higher frequency area controlled by the electron-transfer rate of the materials on the electrode interface, whose diameter is equivalent to the resistance of the charge transfer on the electrode surface (Rct) [26]. Hence, the charge transfer rates of different electrodes were examined by EIS, which was in in 5.0 mM $[Fe(CN)_6]^{4-/3-}$ solution containing 0.1 M KCl. Figure 3 shows that the impedance of bare GCE is the largest and that of Au NPs is the smallest. One reason is that RGO forms an efficient electronic path between electrodes and electrolytes. Another is that Au NPs have good conductivity and enlarges the surface area of Au NPs@RGO, which lead to speed up the conduction of electrons, and reduces the impedance of Au NPs@RGO modified electrodes. These results indicate that the electrode has been successfully modified.

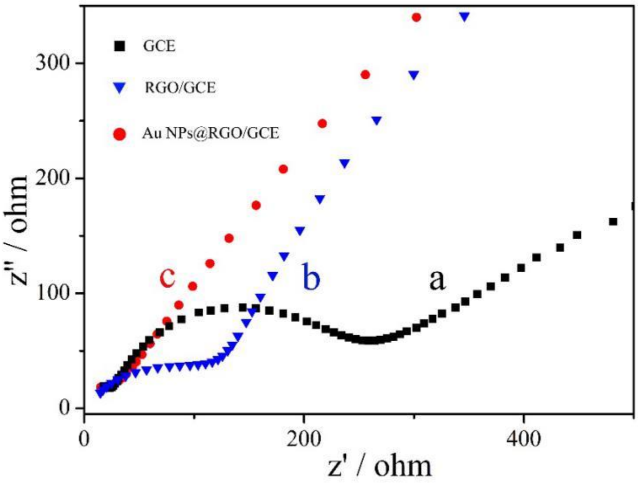

Figure 3. Nyquist plots of electrochemical impedance spectroscopy in 5.0 mM $[Fe(CN)_6]^{4-/3-}$ solution containing 0.1 M KCl. (a) bare GCE, (b) RGO/GCE, (c) Au NPs@RGO/GCE.

3.3 Electrochemical behaviors for Hg^{2+} and Cu^{2+}

Cyclic voltammetric (CV) responses to the bare GCE, RGO/GCE and Au NPs@RGO/GCE electrodes to 1×10^{-5} M Cu^{2+} and 1×10^{-5} M Hg^{2+} were shown in Fig. 4 (0.1 M ABS solution, scan rate of 100 mVs^{-1}). No significant redox peaks can be observed at the curve of bare GCE, and Hg^{2+} appear a weak oxide peak at the RGO/GCE, which means both bare GCE and RGO/GCE cannot determinate Hg^{2+} and Cu^{2+}, simultaneously. While using the Au NPs@RGO/GCE, two independently well-define redox peaks at -0.0655 mV, +0.0036 mV (Cu^{2+}) and +0.261 mV (Hg^{2+}) can be observed obviously, which indicates that CV peaks of Cu^{2+} and Hg^{2+} could be separated completely. These results display that the electrocatalytic activity of Au NPs@RGO/GCE for Cu^{2+} and Hg^{2+} ions is better than that of bare GCE or RGO/GCE.

It also revealed that the Au NPs@RGO/GCE electrode showed a clear enhancement of the peak current. The good electrochemical performance of Hg^{2+} and Cu^{2+} can be contributed to nether reasons. First of all, RGO has excellent electronic conductivity and oxygenated functional groups presenting in RGO could interact with Hg^{2+} and Cu^{2+}, which causes clearly separated redox peaks of Cu^{2+} and Hg^{2+} on the CV curve. Meanwhile, according to equation $I_P = 2.69 \times 10^5 n^{3/2} A D_0^{1/2} v^{1/2} C_0$, the active area of GCE is 0.2232 cm^2, after GCE modified by RGO or Au NPs@RGO, their active areas increased greatly to 0.2678 cm^2 and 0.4018 cm^2, respectively. Moreover, synergistic effect of Au NPs@RGO is more efficient and improve functional properties of modified electrode. Large specific surface area, excellent electrocatalytic activity and synergistic effect ensure favorable performance of Au NPs@RGO/GCE as an electrochemical sensor for sensitive detection of Hg^{2+} and Cu^{2+}.

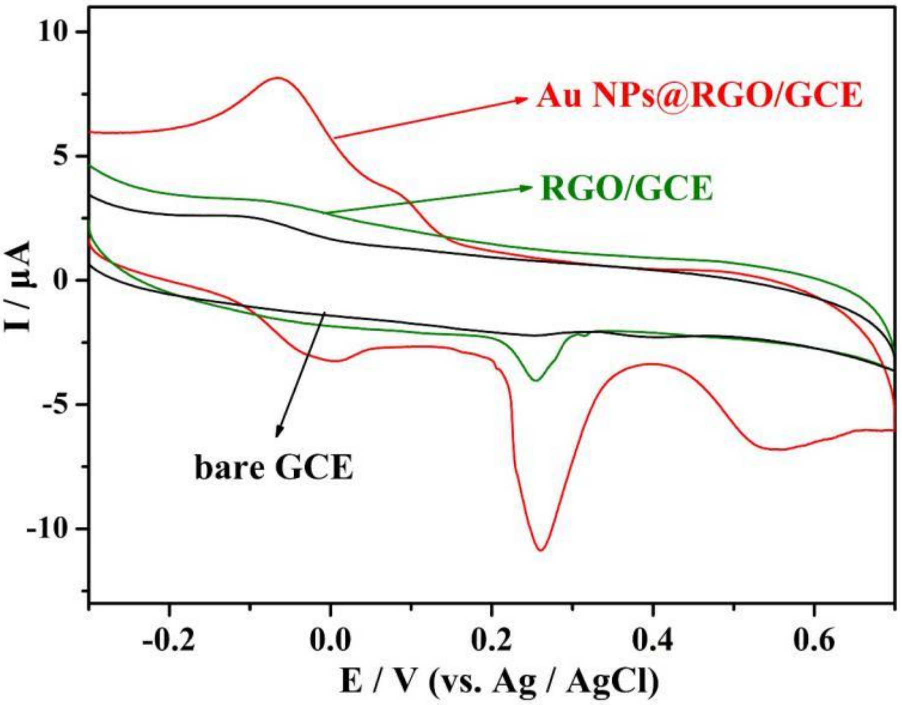

Figure 4. Cyclic voltammograms of different electrodes at 100 mVs^{-1} in 0.1 M ABS (pH=5.0), black line: bare GCE, olive line: RGO/GCE and red line: Au NPs@RGO/GCE.

3.4 Optimization of the experimental parameters

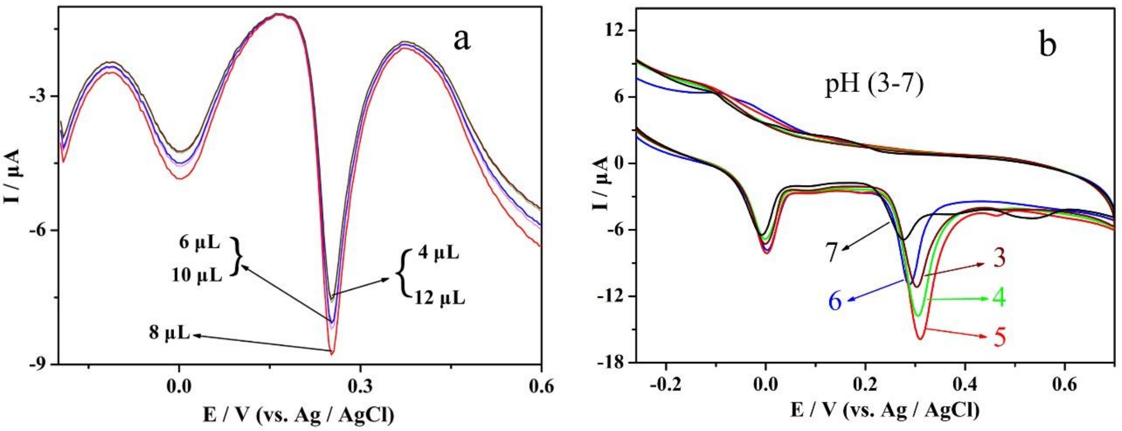

Figure 5. (a) Effect of dosage of Au NPs@RGO. (b) Variety of peaks currents versus pH

In order to achieve the optimum sensitivity for determination of Cu^{2+} and Hg^{2+} ions in Au NPs@RGO/GCE, several experimental parameters were optimized. Fig. 5a displayed the effect of the amount of Au NPs@RGO (4, 6, 8, 10, 12 μL), it is thus clear that redox peak of Cu^{2+} and Hg^{2+} reached the maximum as the amount of Au NPs@RGO was 8 μL.It could be duo to the electron transfer channel and rate of the sensor affected by the number of modified electrode materials [27]. Therefore, 8 μL Au NPs@RGO was used to modify GCE and achieve the highest sensitivity.

Fig. 5b showed electrochemical responses to Cu^{2+} and Hg^{2+} ions at different pH value (ABS 0.1M). It can be seen from the figure that the peak current of the two ions changes obviously with the change of pH value (3~7), but the variation of peak value of $Cu^{2+}$is not as obvious as that of Hg^{2+}, which can be attributed to the fact that the bond forming ability of gold and copper is greater than that of gold and mercury. The electrochemical response of Au-NPs@RGO/GCE to two metal ions is affected by the pH value, the possible reason is that the bonding of Au-NPs is disturbed by excessive hydrogen ions in solutionat lower pH value, while higher pH will affect the hydrolysis state of the two ions. These factors change the magnitude of redox current. Consequently, pH value of 5.0 in 0.1 M ABS was chosen as one of optimal parameters.

3.5 Evaluation of the scan rate

The electrochemical response of the modified electrode to 5×10^{-5} M Cu^{2+} and Hg^{2+} in 0.1 M ABS (pH=5.0) at different scanning rates was investigated. As shown in Figure 6, the redox peak current of Cu^{2+} and Hg^{2+} raised with the increase of scanning rate (20 to 240 mV s^{-1}). The illustration shows that the peak current (I_{pa}) of the two ions had a good linear relationship with the scanning rate, showing that electrochemical catalysis to Cu^{2+} and Hg^{2+} was adsorption-controlled processes. The linear equation can be described as follows, I_{pa} (μA) = 5.7732 − 0.0659 ν (mV s^{-1}) and I_{pc} (μA) = 0.9207 + 0.0632 ν (mV s^{-1}) with the correlation coefficient of 0.997 for Cu^{2+} and I_{pa} (μA) = 0.1952 − 0.1096 ν (mV s^{-1}) with the correlation coefficient of 0.997 for Hg^{2+}.

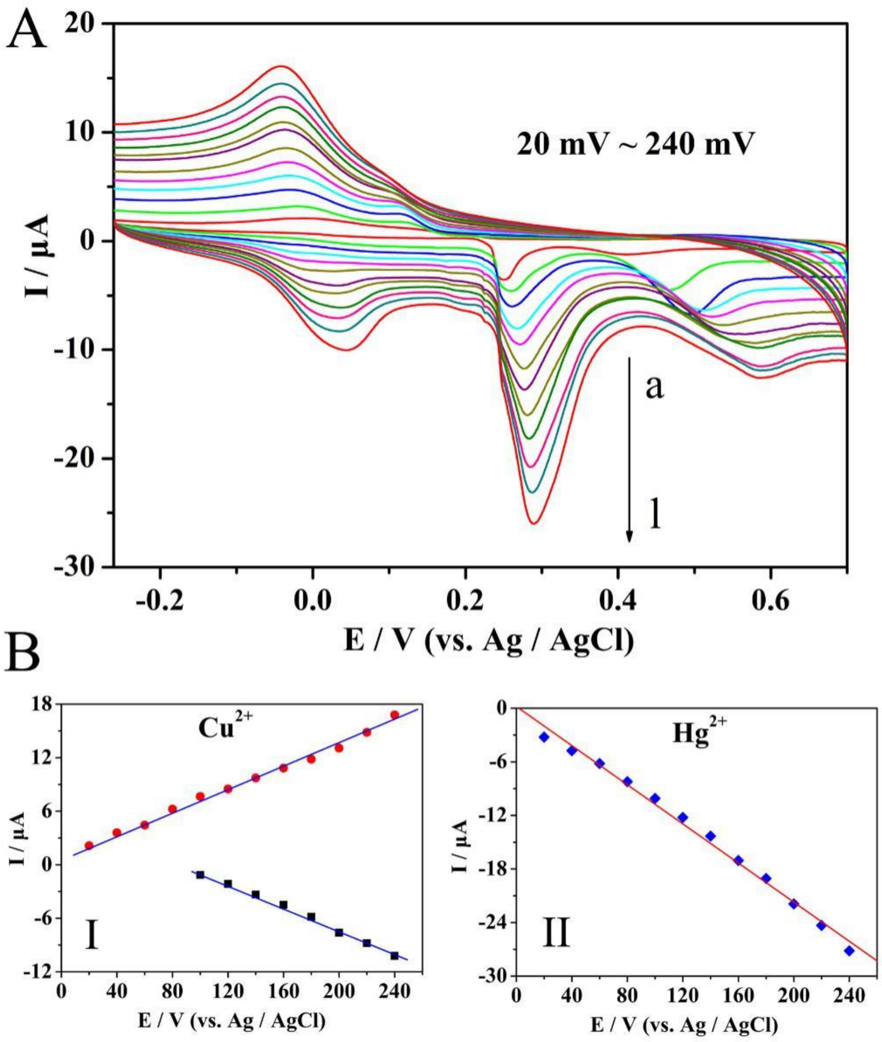

Figure 6. (A) Response of scan rate at Au NPs@RGO/GCE. The scan rate (a–l): 20, 40, 60, 80, 100, 120, 140, 160, 180, 200, 220 and 240 mV s^{-1}. (B) Corresponding linear of peak current towards scan rates for Cu^{2+} and Hg^{2+}.

3.6 Simultaneous determination of Hg^{2+} and Cu^{2+}

With the optimum parameters, we determined Cu^{2+} and Hg^{2+} through keeping the concentration of one ion constant and changing the other ion concentration by DPV duo to its higher detection sensitivity and better resolution. Fig. 7A and Fig. 7B displayed plots of the oxidation peak currents versus 2×10^{-5} M Hg^{2+}/Cu^{2+} (0.05−10 μM) and 2×10^{-5} M Cu^{2+}/Hg^{2+} (0.005−2 μM), which the linear equations were Ipa (μA) = −0.8734−2.3529C (μM) (R=0.9987) and Ipa (μA) = −1.6476−12.3557C (μM) (R=0.9982), respectively. The experimental limits of detection (LOD) were estimated to be 0.02 μM for Cu^{2+} and 0.0015 μM for Hg^{2+}. The results above reveal that when one ion is tested, the other does not interfere, and the two ions can be detected simultaneously. Meanwhile, good linear correlations indicate the stable and efficient electrochemical property of Au NPs@RGO.

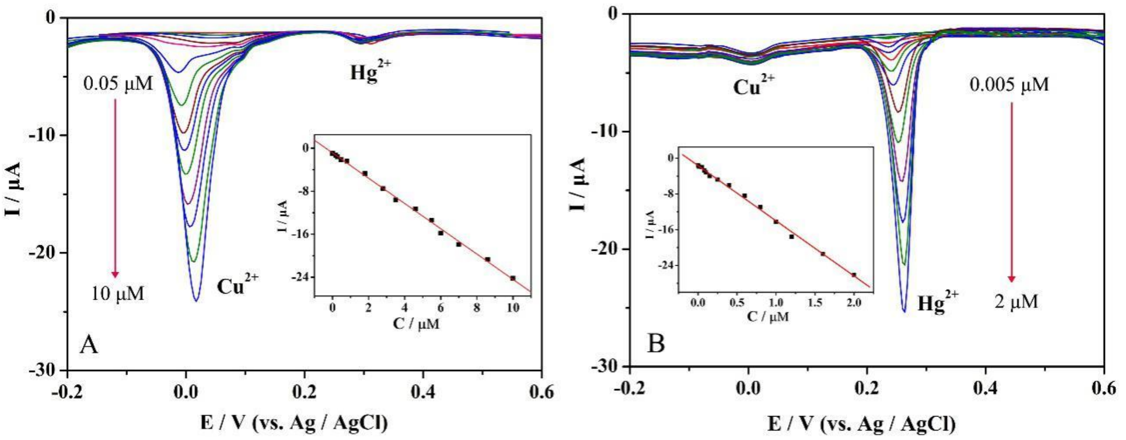

Figure 7. (A) DPV spectrum of 1×10^{-5} M Hg^{2+} and different concentrations of Cu^{2+} (0.05−10 μM). (B) DPV spectrum of 1×10^{-5} M Cu^{2+} and different concentrations of Hg^{2+} (0.005−2 μM). The inserts show plots of peak currents versus concentrations.

LODs and linear ranges of Cu^{2+} and Hg^{2+} ions in present study and some other previous research work are listed in Table 1. It is obvious that LODs obtained by Au NPs@RGO/GCE are far lower than those achieved by other work. Thus, Au NPs@RGO/GCE can be used as a new sensor proposed to detect Cu^{2+} and Hg^{2+}. The results further indicate that RGO adsorbs a large number of Au nanoparticles and chelates with them in our work. Au nanoparticles have good conductivity [28] and high concentration of defect produced during the nonequilibrium process [29], which make them have better electrocatalytic activity.

Table 1. Comparison of the analytical performance for detection of Cu^{2+} and Hg^{2+}

Electrode	Linear range (μM)		Detection limit (μM)		References
	Cu^{2+}	Hg^{2+}	Cu^{2+}	Hg^{2+}	
SNAC	0.09-4.8	0.09-0.99	0.0232	0.0246	30
Fe_3O_4	0.1-1.0	0.1-10.0	0.0221	0.0587	31
$Pd_{1.5}$/PAC-900	0.5-5.0	0.24-7.5	0.066	0.054	32
$MnFe_2O_4$@Cys	0.4-1.8	1.4-3.0	0.0626	0.208	33
EDTA-PANI/SWCNTs/SS	1.2-2000	2-200	0.08	0.68	34
Au NPs@RGO	0.05−10	0.005−2	0.02	0.0015	This work

3.7 Reproducibility, stability and selectivity

To verify the reproducibility of modified electrodes, Cu^{2+} and Hg^{2+} mixed solution was continuously detected by DPV with the same electrodes. The relative standard deviations were as follows, 2.25% and 1.68%, respectively. Furthermore, the stability of Au NPs@RGO/GCE was also appraised. After two weeks of storage, the modified electrode was used to detect two ions. The peak current decreased by only 4.26% and 3.27% for Cu^{2+} and Hg^{2+} compared with original current. It illustrated the excellent reproducibility and stability of Au NPs@RGO/GCE.

In addition, the anti-interference ability of Au NPs@RGO/GCE was evaluated. Adding some other ions, such as Cd^{2+}, Fe^{3+}, Co^{2+}, Pb^{2+} (1×10^{-4} M), and Na^{+} (5×10^{-4} M) to Cu^{2+} and Hg^{2+} solution, Figure 8 shows the negligible effects of these ions toward the initial peak current, indicating that Au NPs@RGO/GCE has a high selectivity for the detection of two ions.

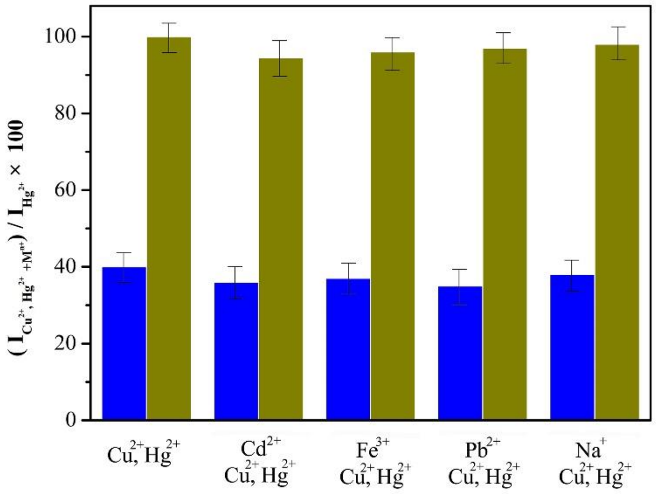

Figure 8. Response of stripping current signals of Cu^{2+} and Hg^{2+} at Au NPs@RGO/GCE (adding Cd^{2+}, Fe^{3+}, Pb^{2+} (1×10^{-4} M), and Na^{+} (5×10^{-4} M), respectively).

3.8 Sample analysis

Table 2. Detection results for real samples.

Sample		Determination (μM)		Added (μM)		Total		Recovery (%)		RSD (%)	
		Cu^{2+}	Hg^{2+}	Cu^{2+}	Hg^{2+}	Cu^{2+}	Hg^{2+}	Cu^{2+}	Hg^{2+}	Cu^{2+}	Hg^{2+}
River water	1	0.00	0.00	1.00	1.00	0.963	1.005	96.3	100.5	1.8	1.6
	2	0.00	0.00	2.00	2.00	2.024	2.068	101.2	103.4	1.5	0.7
	3	0.00	0.00	3.00	3.00	3.038	2.978	101.3	99.3	1.1	1.2
Tap water	1	0.00	0.00	1.00	1.00	1.017	1.008	101.7	100.8	2.7	1.5
	2	0.00	0.00	2.00	2.00	1.965	1.928	98.25	96.4	1.6	0.5
	3	0.00	0.00	3.00	3.00	3.014	2.912	100.5	97.1	0.9	1.2

To achieve the applicability of proposed sensor, water samples collected from local tap water and Yangtze River were detected by DPV. Before measurement, water samples were treated with 0.1 ABS (pH 5.0). At the beginning, no obvious signals were examined in water samples. Then, known concentrations of Cu^{2+} and Hg^{2+} were added to the samples, and the analysis results were shown in Table 2. The recoveries were 96.3-101.7% for Cu^{2+} and 96.4-103.4% for Hg^{2+}, respectively. Relative standard deviation were all below 5%. It can be concluded that Au NPs@RGO/GCE has potential application value in electrochemical detection of heavy metal ions.

4. CONCLUSIONS

In this work, Au NPs@RGO nanocomposite was successfully developed by a facile method. Au NPs@RGO modified electrode showed excellent electrochemical performance for Cu^{2+} and Hg^{2+} due to good conductivity of Au nanoparticles, high surface-to-volume ratio and synergistic effect of Au NPs@RGO. Compared to previously prepared sensors, Au NPs@RGO/GCE exhibits particularly low detection limits of 0.02 μM and 0.0015 μM for Cu^{2+} and Hg^{2+}. And the new sensor had a high stability, reproducibility and anti-interference properties, which provides a reliable and effective method for the determination of Cu^{2+} and Hg^{2+}. The current work improves a potential method for the preparation of sensing materials and the design of new electrochemical sensors for the detection of Cu^{2+} and Hg^{2+}, even other metal ions.

ACKNOWLEDGMENTS
The author gratefully acknowledge the financial support from Wuhu Institute of Technology (wzyzrzd201703) and Department of Education Anhui Province (KJ2018A0696). The author also thanks Professor, Ph.D. supervisor Zhousheng Yang, Professor Kunhong Hu, and Dr. Jun Liu for their assistance.

References

1. D.Q. Cao, X. Song, X.M. Fang, W.Y. Yang, X.D. Hao, E. Iritanib and N. Katagiri, *Chem. Eng. J.*, 354 (2018) 866.
2. Y. Xun, L. Feng, Y.D. Li and H.C. Dong, *Chemosphere*, 189 (2017) 161.
3. J. Aaseth, B. Hilt and G.Bjørklund, *Environ. Res.*, 164 (2018) 65.
4. P.C. Zhang, Z.Z. Lyu, J. Viktorova, A.Offenhäusser and D. Mayer, *Biosens. Bioelectron.*, 117 (2018) 450.
5. C. S.Vergilio, C. E. V. Carvalho and E.J.T. Melo, *Toxicol. in Vitro,* 29 (2015) 63.
6. P. Mahato, S. Saha, P. Das, H. Agarwalla and A. Das, *RSC Adv.,* 4 (2014) 36140.
7. M. Wang, F. Yan, Y. Zou, L. Chen, N. Yang and X. Zhou, *Sensor Actuat B-Chem.,* 192 (2014) 512.
8. W. Wang, Y. Zhang, Q. Yang, M. Sun, X. Fei, Y. Song, Y. Zhang and Y. Li, *Nanoscale,* 5 (2013) 4958.
9. D. Guo, Z. Dong, C. Luo, W. Zan, S. Yan and X. Yao, *RSC Adv.,* 4 (2014) 5718.
10. O.T. Butler, W.R.L. Cairns, J.M. Cook and C.M. Davidson, *J. Anal. Spectrom.,* 27 (2012) 187.
11. P. Ndokoye, J. Ke, J. Liu, Q. D. Zhao and X. Y. Li, *Langmuir,* 30 (2014) 13491.
12. Z. Qing, Z. Mao, T. Qing, X. He, Z. Zou, D. He, H. Shi, J. Huang, J. Liu and K. Wang, *Anal. Chem.,* 86 (2014) 11263.
13. X. Xu, G. Duan, Y. Li, G. Liu, J. Wang, H. Zhang, Z. Dai and W. Cai, *ACS Appl. Mater. Interfaces*, 6 (2014) 65.
14. J. Huang, X. Gao, J. Jia, J.-K. Kim and Z. Li, *Anal. Chem.* 86 (2014) 3209.
15. P.K. Sahoo, S. Sahoo, A.K. Satpati and D. Bahadur, *Electrochim. Acta,* 180 (2015) 1023.
16. D. Chen, H. Feng and J. Li, *Chem. Rev.,* 112 (2012) 6027.
17. J. Ping, Y. Wang, K. Fan, J. Wu and Y. Ying, *Biosens Bioelectron.,* 28 (2011)204.
18. J. Li, J. Yang, Z. Yang, Y. Li, S. Yu and Q. Xu , *Anal Methods,* 4 (2012) 1725.
19. N. Zhou, J. Li, H. Chen, C. Liao and L. Chen, *Analyst,* 138 (2013) 1091.
20. X.C. Dong, W. Huang and P. Chen, *Nanoscale. Res. Lett.,* 6 (2011).
21. J. Li, C. Y. Liu and Y. Liu, *J. Mater. Chem.,* 22 (2012) 8426.
22. P.K. Sahoo, Bharati Panigrahy, S. Sahoo, A.K. Satpati, Dan Li and D. Bahadur, *Biosens Bioelectron.,* 43 (2013) 293.
23. W.S. Hummers and R.E. Offeman, *J. Am. Chem. Soc.,* 80 (1958) 1339.

24. S.J. Xu, L. Yong and P.Y. Wu, *ACS Appl. Mater. Interfaces,* 5 (2013) 654.
25. H. M. Song, D. H. Anjum and N. M. Khashab, *RSC Adv.,* 2 (2012) 3621.
26. C. Li, W. Liu, Y. Gu, S. Hao, X. Yan, Z. Zhang and M. Yang, *J. Appl. Electrochem.,* 44 (2014)1059.
27. J. Zhou , X. Li, L.L. Yang, S.L. Yan, M.M.Wang, D.Cheng, Q. Chen, Y.L. Dong, P. Liu, W.Q. Cai and C.C. Zhang, *Anal. Chim. Acta,* 899 (2015) 57.
28. I. Streeter, R. Baron and R.G. Compton, *J. Phys. Chem. C* 111 (2007)17008.
29. K.V. Anikin, N.N. Melnik, A.V. Simakin, G.A. Shafeev, V.V. Voronov and A.G. Vitukhnovsky, *Chem. Phys. Lett.,* 366 (2002) 357.
30. R. Madhu, K.V. Sankar, S.M. Chen and R.K. Selvan, *RSC Adv.,* 4 (2014) 1225.
31. W.J. Li, X.Z. Yao, Z. Guo, J.H. Liu and X.J. Huang, *J. Electroanal. Chem.,* 749 (2015) 75.
32. P. Veerakumar, V. Veeramani, S.M. Chen, R. Madhu and S.B. Liu, *ACS Appl. Mater. Interfaces,* 8 (2016) 1319.
33. S.F. Zhou, J.J. Wang, L. Gan, X.J. Han, H.L. Fan, L.Y. Mei, J. Huang and Y.Q. Liu, *J. Alloys Compd.,* 721 (2017) 492.
34. M.A. Deshmukh, R. Celiesiute, A. Ramanaviciene, M.D. Shirsat and A. Ramanavicius, *Electrochim. Acta.* 259 (2018) 930.